Available online at www.sciencedirect.com
ScienceDirect
Journal of Electrostatics 66 (2008) 107–114
Journal of ELECTROSTATICS
www.elsevier.com/locate/elstat

Electric wind induced by sliding discharge in air at atmospheric pressure

E. Moreau*, C. Louste, G. Touchard

Laboratoire d'Etudes Aérodynamiques, UMR 6609 CNRS, Groupe Electrofluidodynamique, Université de Poitiers, 86962 Futuroscope-Chasseneuil, France

Received 26 June 2006; received in revised form 25 June 2007; accepted 29 August 2007
Available online 16 October 2007

Abstract

This paper deals with an experimental study about the electric wind induced by three different surface discharges based on dielectric barrier discharges and sliding discharges, at atmospheric pressure in ambient air. These discharges are established between two or three electrodes, flush mounted at the wall of a flat plate. A typical industrial application of such surface discharges may be, for instance, airflow control, because they may be used as an air-moving actuator, usually called "plasma actuator". First, the electrical current of these different discharges is analyzed. Secondly, the time-averaged velocity of the electric wind produced by each discharge is measured with a Pitot tube sensor. Then, their effect on the boundary layer of a low-velocity airflow is studied by particle image velocimetry (PIV).

Keywords: Electric wind; Surface sliding discharge; DBD; Corona

1. Introduction

Several studies have shown that the electric wind produced by non-thermal surface plasmas may be used for airflow control [1]. In our laboratory, two types of surface discharges are usually used as plasma actuators. The first one is a DC surface corona discharge. This DC discharge, which is usually established between two wires flush mounted at the wall of a dielectric, can produce an electric wind velocity up to 5 m/s. The produced electric wind, which flows tangentially to the wall, has shown its efficiency for airflow control in various aerodynamic conditions (for instance [1–3]). But the main drawback of this discharge is that it becomes unstable under certain atmospheric conditions. For instance, corona-to-arc transition appears when the relative air humidity exceeds a certain threshold. The second type of discharge is the dielectric barrier discharge usually called "DBD". It seems that this discharge has been first perfected at atmospheric pressure in air by Masuda and Washizu [4] for ionic charging of particles. Roth used it for the first time for airflow applications at the end of the 1990s [5]. It is now the most used discharge for airflow control [6–8]. Typically, it can generate an ionic wind up to about 7 m/s [9]. Nevertheless the plasma area extension is limited to about 2 cm. This might be a crucial drawback for large-scale applications.

Consequently, we have recently perfected a new type of electrode configuration, which consists of a three-electrode geometry [1,10]. This geometry is based on the device used to produce "sliding discharge", initially developed in pure gas for others applications [11,12]. The sliding discharge in air has the advantage of producing wide plasma sheet, which might allow large-scale applications, and this discharge is very stable, whatever the environmental conditions.

This paper deals with the electric wind induced by DBDs, established with the well-known two-electrode geometry (this actuator is usually called *single* DBD actuator), and with a new geometry based on a three-electrode configuration.

First, the electrical current of these discharges is discussed. Secondly, the electric wind induced by each discharge is measured with a Pitot tube, in order to plot time-averaged velocity profiles. In the last part of the present paper, the effect of these discharges on the boundary layer of a 5 m/s airflow is characterized by particle image velocimetry (PIV).

*Corresponding author. Tel.: +33 5 49 49 69 40; fax: +33 5 49 49 69 68.
E-mail address: eric.moreau@lea.univ-poitiers.fr (E. Moreau).

0304-3886/$ - see front matter © 2007 Elsevier B.V. All rights reserved.
doi:10.1016/j.elstat.2007.08.011

2. Experimental setup

Two experimental setups have been used to produce both different discharges. The single DBD actuator is based on a two-electrode geometry (Fig. 1a). Electrodes (1) and (2) are placed on each side of a Plexiglas (PMMA) plate. The electrode placed below the dielectric plate is encapsulated with an epoxy resin. Electrode (2) is grounded while electrode (1) is excited by a sine high voltage V_{AC} generated here by a TREK 20/20C power amplifier (20 mA, 20 kHz). In such conditions, a surface plasma sheet of a few millimeters wide is generated on the upper side of the plate and close to the AC electrode (1), as illustrated by the top-view picture of the plasma in Fig. 1b. The electric wind flows tangentially to the wall, as illustrated by the arrow in Fig. 1a.

The second geometrical setup is similar to the first one but a third electrode is added above the plate (electrode (3) in Fig. 2a). Electrode (1) is still supplied by an AC high voltage, but electrodes (2) and (3) are excited by a DC high voltage V_{DC}, with the help of a DC power supply DEL ($\pm$40 kV, 3.75 mA). This DC component may be positive or negative. In one hand, if V_{DC} is negative, then a wide and luminous plasma sheet is visible between electrodes (1) and (3), as illustrated by Fig. 2b. In the other hand, if V_{DC} is positive, the visible plasma sheet is not modified, and it is still as illustrated by Fig. 1b.

All electrodes are aluminum foils ($\approx$15-μm thick, 10-mm wide, 200-mm long) stick on the surface of a PMMA flat plate (4-mm thick, 200-mm wide and 300-mm long). The currents I_2 and I_3 are measured with a 1 kΩ shunt resistor connected to a 1 MHz oscilloscope. The gap between electrodes (1) and (3) is here equal to 40 mm.

3. Electrical current measurements

In this section, measurements of the different currents (I_2 and I_3) of every discharge are presented and discussed.

3.1. Dielectric barrier discharge

Here, experiments are conducted in using the two-electrode device presented in Fig. 1a. Electrode (2) is grounded and the other one is connected to a sine high voltage V_{AC} of several kV and a frequency of 1 kHz. In such conditions, the amplitude of V_{AC} to ignite the plasma must be greater than 8 kV (16 kV_{p-p}). Then, above 8 kV, a plasma sheet of blue ionized air is visible on the surface of the dielectric and starting from the AC electrode (1). It appears visually to be a quasi-uniform glow, but, in fact, it consists of micro discharges distributed uniformly in time and space along the electrode length. The plasma extension increases with V_{AC}, and depends on the surface conductivity, but it is limited to a maximum value of about 20 mm [9]. For example, Fig. 3a presents a typical behavior of the applied voltage and the associated discharge current versus time, for an AC sine voltage V_{AC} of 20 kV at 1 kHz.

The current is composed of two components: a capacitive component plus the discharge current. The capacitive component is a sine component with a phase shift of $\pi/2$ compared to the voltage. It is due to the dielectric between the upper electrode and the lower one (capacitor geometry). This capacitive component is determined by measuring the capacitor before the plasma ignition. Here, its amplitude is about 2 mA. If the capacitive current is removed, we obtain only the discharge current (Fig. 3b). This one consists in current pulses,

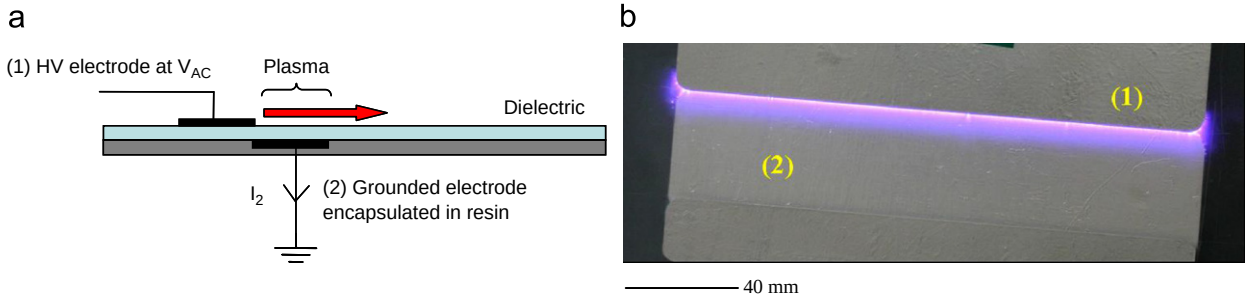

Fig. 1. Schematic side view of the dielectric barrier discharge device (a) and picture (top view) of the induced visible plasma (b).

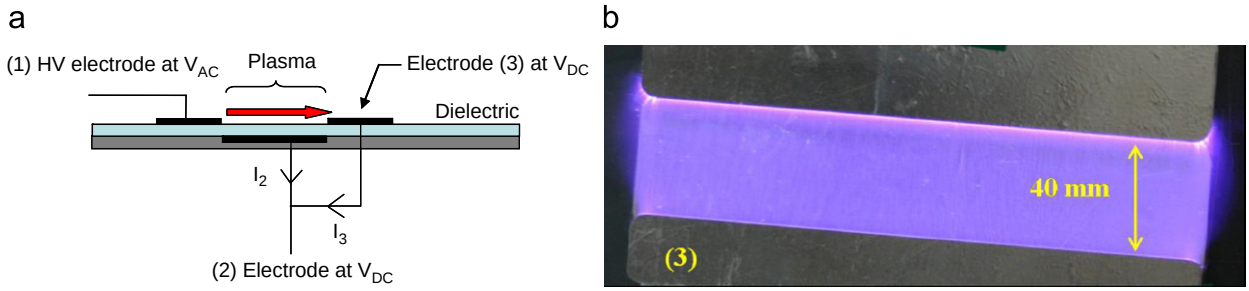

Fig. 2. Schematic side view of three-electrode device (a) and picture (top view) of the extended plasma when V_{DC} is negative (b).

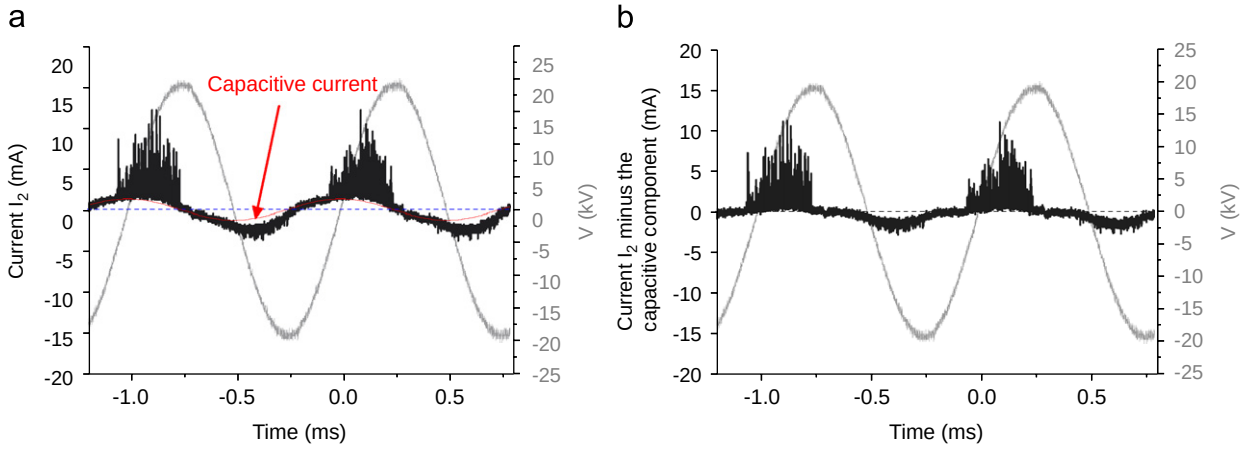

Fig. 3. Typical behavior of the total current I_2 (a) and DBD discharge current (b).

corresponding to micro discharges or streamers. These pulses are not symmetric. The positive ones are short (about 1 μs) and rather high (between 5 and 10 mA) but relatively sparse. It seems that each current peak corresponds to a streamer. More, there is a synchrone current, which corresponds to the low-velocity drift of ions between two successive streamers. The amplitude of negative pulses is three times smaller (2.5 mA) than the positive ones but the number of negative pulses is three times more important. This shows that the discharge occurring during the negative half-cycle is more homogeneous than the positive one. The time-averaged current is equal to zero.

At a so low frequency, one of our previous works [9] has shown that DBD seems to be composed of a positive corona and a negative corona discharge that act alternately during the positive and the negative half-cycle, respectively. Non-stationary measurements of the induced ionic wind had been performed by laser Doppler velocimetry (LDV) system with synchronized records of electrical current and instantaneous velocity. These experiments had shown that the negative discharge induced more velocity than the positive one [9].

3.2. Discharge in three-electrode configuration with $V_{DC}<0$

This section presents the discharges obtained with the three-electrode device. Electrode (1) remains connected to a sine high voltage. Electrodes (2) and (3) are connected to the same negative DC power supply. We call $V = V_{AC} - V_{DC}$. The discharge obtained in such conditions is called "sliding discharge" because it looks like the plasma obtained with the sliding discharges initially perfected by Arad et al. [11] with fast-rising pulsed voltages. However, electrical and environmental conditions were completely different.

Fig. 4 presents a typical behavior of the discharge currents versus time when the AC voltage V_{AC} is a sine voltage of 20 kV at 1 kHz and the DC voltage V_{DC} applied on electrodes (2) and (3) is −5 kV. This value is rather low. Voltages up to −10 kV may be applied without spark. In such conditions, the sliding discharge generates a large blue plasma sheet on the upper side of the dielectric. It covers the dielectric surface between electrodes (1) and (3), as illustrated in Fig. 2b. The current I_3 measured on electrode (3) is presented in Fig. 4a. We observe some small positive pulses (2 mA) when V becomes positive. Greater positive pulses (up to 20 mA) can be observed when V reaches about 20 kV. These pulses correspond to the sliding discharge current, i.e. the current due to the drift and the slide of the positive ions created at electrode (1) by the BDB, towards electrode (3) because its polarity is negative. It seems that each current peak corresponds to a streamer. In practice, the plasma sheet composed of these streamers is visible only when the important positive pulses are present. During the negative half-cycle, current I_3 is equal to zero because the negative ions created by electrode (3) are not attracted by electrode (3).

Fig. 4b shows the current I_2. This current is composed by three components:

- A sine capacitive component (1.5 mA of amplitude) which has been removed here.
- A DBD component composed of positive and negative pulses. These two components are called "positive and negative DBD pulses" in Fig. 4b. It has been experimentally verified that this component corresponds to the DBD current, as presented in Fig. 3b. However, here, these pulses are lightly smaller than those presented in Fig. 2b, more especially in the negative half-cycle. This is due to the fact that the negative polarity of electrode (3) results in a decrease of the DBD intensity during this negative half-cycle.
- The last component is composed of important negative pulses (up to −15 mA). These pulses, called "sliding pulses" in Fig. 4b are symmetrical to the pulses measured on electrode (3) but with an opposite sign. It seems that this current is due to the image charges of the sliding current I_3.

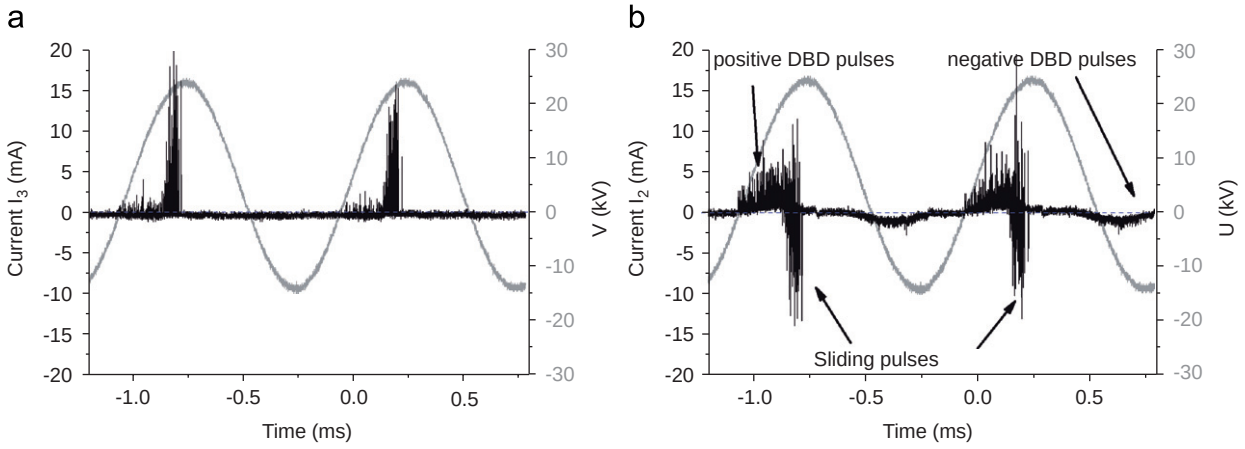

Fig. 4. Current versus time of a sliding discharge ($V_{DC}<0$): current I_3 measured at electrode (3) (a) and current I_2 measured at electrode (2) (b).

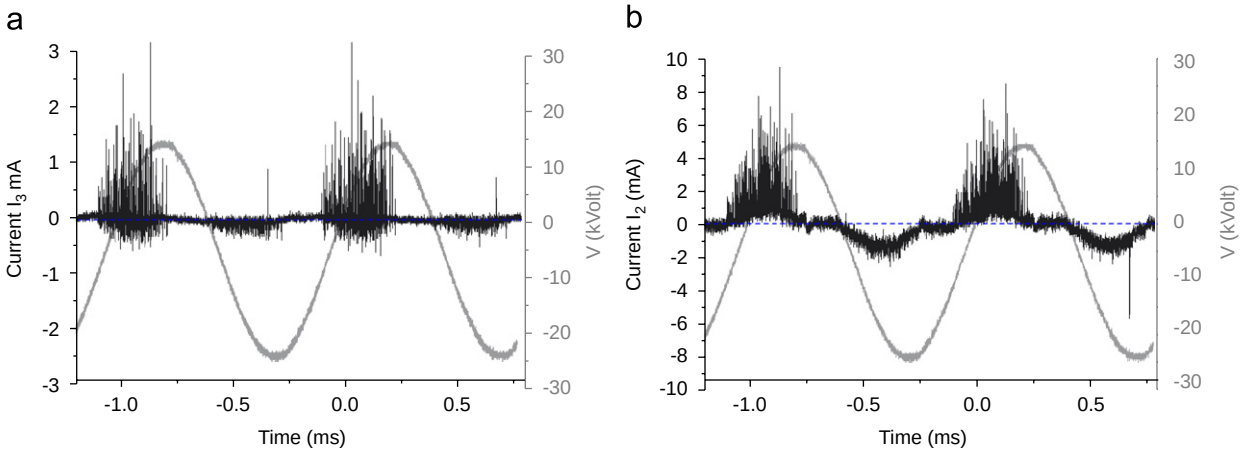

Fig. 5. Current versus time obtained with the three-electrode device when $V_{DC}>0$: I_3 (a) and I_2 (b).

How to interpret these curves? In fact, it seems that a typical DBD occurs, due to the AC HV between electrodes (1) and (2). During the positive half-cycle, it plays the role of an "ionizer", that produces positive ions, such as in a positive corona. Then, because of the negative polarity of electrode (3), and above a threshold of about 20 kV here (corresponding to a reduced electric field of 20 kV divided by 4 cm, i.e. 5 kV/cm), the positive ions slide from electrode (1) towards electrode (3). This positive ion motion induces the positive peaks of current I_3 in Fig. 4a. During the negative half-cycle, it seems that no charge are transferred from electrodes (1) to (3), because electrode (3) is negative. More, the DBD current is limited. Indeed, the negative current of Fig. 4b is lower than the one of Fig. 3b. This point will be confirmed by velocity measurements. We can then consider that the sliding discharge is a mix between an AC DBD and a corona discharge. With our device, the amplitude of the AC HV must be greater than 8 kV to ignite the DBD. The amplitude of V (maximum voltage between electrodes (1) and (3)) has to be greater than 20 kV to obtain a sliding discharge with a negative DC source.

3.3. Discharge in three-electrode configuration with $V_{DC}>0$

Here a sine HV signal is still applied to electrode (1). Electrodes (2) and (3) are now connected to a positive DC voltage. The obtained discharge established in such conditions is not clearly a sliding discharge. Indeed, there is no luminous plasma sheet as illustrated in Fig. 2b. This discharge looks like a dielectric barrier discharge, as shown in Fig. 1b.

Fig. 5 illustrates a typical behavior of the current versus time when the AC sine voltage V_{AC} has an amplitude of 20 kV and the DC voltage V_{DC} applied to electrodes (2) and (3) is equal to 5 kV. Figs. 5a and b present the currents I_3 and I_2, respectively. A capacitive component is also measured (amplitude 1.5 mA) on I_2 but it has been removed in Fig. 5b.

In one hand, the current I_2 is nearly similar to the DBD current presented in Fig. 3b. This shows that there is still a DBD discharge between electrodes (1) and (2). In the other hand, it is more difficult to interpret the behavior of current I_3. When the voltage V increases from its mean value to

15 kV, the current consists of positive and negative pulses. Positive pulses are more important and sparser than the negative ones. In one hand, it seems that a part of the positive ions created by the DBD during the positive half cycle of V_{AC} slide from electrode (1) towards electrode (3). However, this phenomenon is weaker than in the case of a sliding discharge ($V_{DC}<0$) because the polarity of electrode (3) is here positive, and the electric field is then lower. In the other hand, it seems that positive ions are created at electrode (3), and drift from electrodes (3) to (1). This may explain the negative pulses of current I_3 during the positive half-cycle of V_{AC}.

4. Electric wind measurements

The electric wind produced by these three different discharges is measured with the help of a Pitot tube. This 1-mm diameter tube is made in glass to avoid interaction with the plasma. Measurements are conducted at the middle of the plate span wise. The coordinate system (x,y)

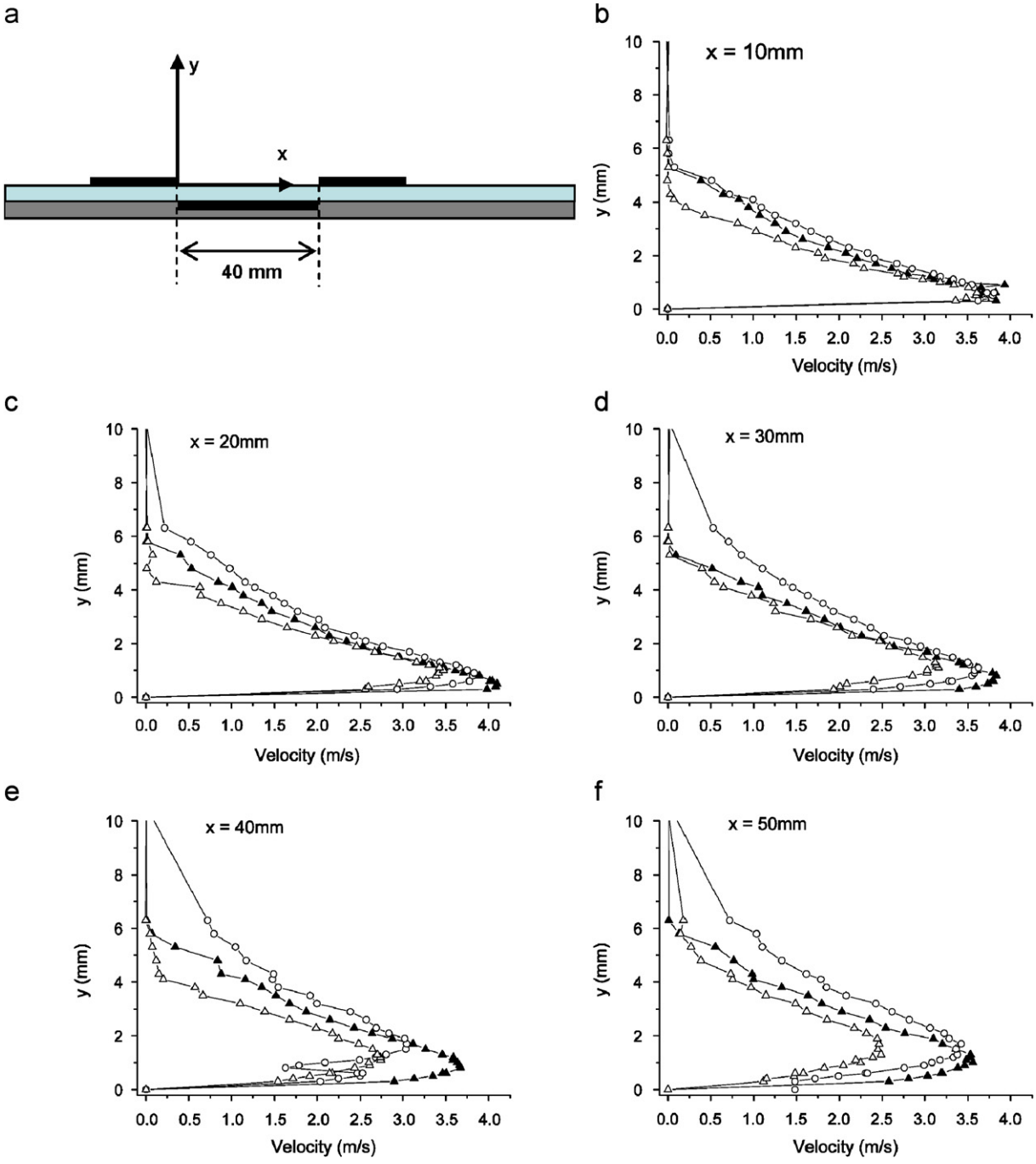

Fig. 6. Electric wind time-averaged velocity profiles induced by the three discharges at different x-values: dielectric barrier discharge (-▲-), sliding discharge with $V_{DC} = -10$ kV (-△-) and discharge with $V_{DC} = +19$ kV (-○-).

is presented in Fig. 6a. The x component of the velocity is measured at five x positions (from $x = 10$–50 mm). The AC voltage V_{AC} remains a sine voltage (20 kV, 1 kHz). The DC positive and negative voltages applied at electrodes (2) and (3) have been increased up to the breakdown voltage, i.e. +19 and −10 kV, respectively.

The time-averaged value of the electric wind velocity of the three discharges is presented in Fig. 6. Each velocity

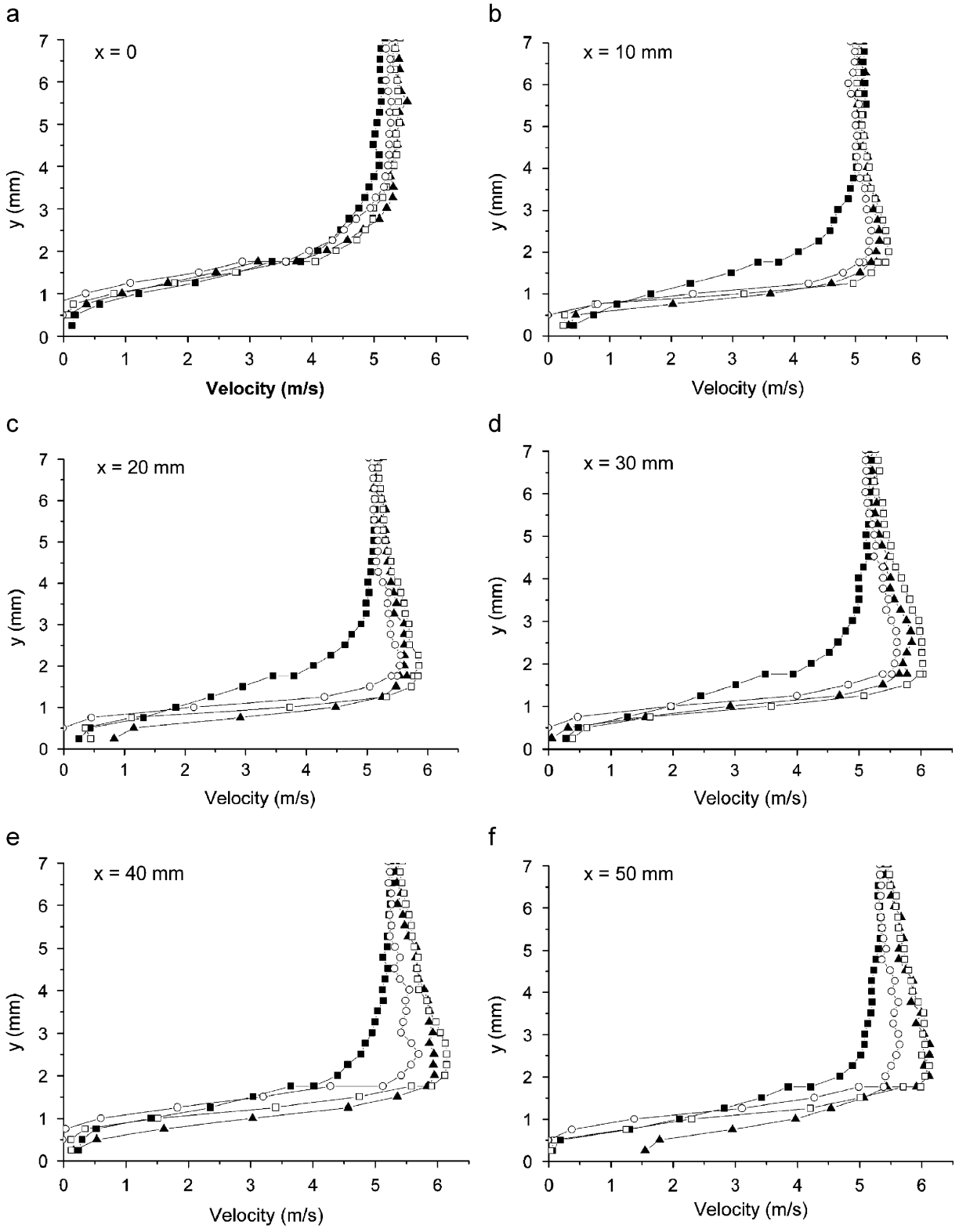

Fig. 7. Time-averaged velocity profiles of a 5 m/s airflow boundary layer: baseline (-■-) , and manipulated by a dielectric barrier discharge (-▲-), a sliding discharge with $V_{DC}<0$ (-○-) and a discharge with $V_{DC}>0$ (-□-).

measurement corresponds to a data record of 3 s at 1 kHz. The shape of the velocity profiles shows that the discharges induce an ionic wind of several m/s tangentially to the plate wall. The height of the air flow layer is about 6 mm. From $x = 20$–50 mm, the ionic wind slowly decreases and separates from the plate wall. At $x = 10$ mm (Fig. 6b), the three discharges have about the same maximum velocity (≈ 4 m/s). This maximum velocity value is obtained at a height of about 0.5 mm above the wall. The three discharges have nearly a similar effect at this place, because the three discharges act as a DBD discharge from $x = 0$–10 mm. Downstream $x = 20$ mm, the ionic wind produced by the DBD is the fastest. It is also closer to the surface than the two other ones. Furthermore, the velocity of the electric wind created by the three-electrode device with $V_{DC} > 0$ is always greater than when $V_{DC} < 0$. When $V_{DC} > 0$, the velocity at about 1 mm above the wall ($y = 1$ mm) is smaller than in the case of a DBD, but the velocity is greater for $y \geqslant 2$ mm.

All these results agree with the explanations given in the previous section concerning the current behavior of these discharges. As indicated in one of our previous works [9], the DBD is composed of successive positive and negative coronas, at least when the voltage frequency is low (≈ 1 kHz). More, we had shown that the negative discharge (occurring during the negative half-cycle of V_{AC}) resulted in a faster velocity than the positive one. Consequently, the velocity profiles induced by the discharges established with the three-electrode device may be explained as follows. In one hand, when V_{DC} is positive, the negative space charge created by the DBD during the negative half-cycle is more accelerated, resulting in a faster time-averaged velocity. In fact, the negative corona is enhanced, in spite of the positive one. On the other hand, when V_{DC} is negative, the effect is reversed, and the velocity is lower. However, the three-electrode device does not allow here to increase the electric wind velocity because the ionization at electrode (3) induces a counter electric wind. This phenomenon is particularly illustrated by Fig. 5e. Indeed, the sudden decrease in velocity at $x = 40$ mm (left edge of electrode (3)) and $y = 0.9$ mm is due to positive ions created at electrode (3), and repulsed because the positive polarity of this electrode.

5. Effect on a boundary layer

We are now going to study the effect of each discharge on the boundary layer of a 5 m/s airflow along a flat plate placed in a wind tunnel. The airflow is characterized by PIV. The PIV measurements are realized with a LAVISION system (1280×1024 pixel camera, Yag–Nd laser of 532 nm). Images are computed in using cross-correlation between two frames with a window of 32×32 pixels, and an overlap of 50%.

Fig. 7 presents different time-averaged velocity profiles of the flow, obtained by PIV, at several x-locations, for the three discharges. Only the horizontal component is presented here, in order to be able to compare with the Pitot tube measurements.

The boundary layer has been tripped 10 cm upstream the actuator location and then it has a typical turbulent boundary layer shape. Its height is 3 mm. At position $x = 0$ mm, the three discharges have no visible effect on the horizontal component of the flow. In fact, the discharges induce a depression here, resulting in a negative vertical component (toward the wall).

At $x = 10$ mm, the effect of the three discharges is rather similar but it seems that the maximum effect is obtained when $V_{DC} > 0$. The velocity increases up to 5.5 m/s at 1.5 mm above the wall. More, it increases of about 3 m/s (from 1 to 4 m/s) at about 1 mm above the surface. At a distance greater than 1 mm above the wall, the discharge based on the three-electrode device with $V_{DC} > 0$ produces the most efficient effect. All these results are in agreement with the electric wind measurements presented in Fig. 6: the DBD produced the fastest velocity, close to the wall. When $V_{DC} > 0$, the velocity is lightly lower, and less close to the wall ($y > 1$ mm).

6. Conclusion

In the present paper, a new three-electrode geometry device to produce large-scale surface plasma actuators has been presented. The induced discharges have been studied electrically and mechanically. It has been shown that the AC surface DBD established usually by the single plasma actuator device may be modified, by adding a third electrode that allows to bring a DC component to the applied high voltage. The three main remarks concerning the discharge produced by the three-electrode device are:

- It seems that the DBD plays the role of a "ionizer".
- The DC component allows to enhance the ion slide by streamer propagation along the dielectric wall.
- The discharge characteristics depend strongly on the polarity (positive or negative) of the DC electrode.

In one hand, in the conditions used here, the third electrode did not allow to accelerate significantly the electric wind produced by the single DBD actuator. This is due to a counter ionic wind produced at the DC electrode because the electric field is too high. On the other hand, other experiments have been being conducted since the experiments illustrated in the present paper. In decreasing the AC high voltage and increasing its frequency, we have shown that the three-electrode device allowed to accelerate strongly the electric wind velocity produced by a DBD with a smaller electrical power consumption. These results will be published very soon.

Furthermore, the sliding discharge produced when $V_{DC} < 0$ might be used for others large-scale applications, such as industrial air decontamination, for instance. Some experiments will be conducted very soon in this way in our laboratory.

References

[1] E. Moreau, Airflow control by non thermal plasma actuators, J. Phys. D 40 (2007) 605–636.
[2] R. Sosa, G. Artana, E. Moreau, G. Touchard, Stall control at high angle of attack with plasma sheet actuator, Exp. Fluids 42 (2007) 143–167.
[3] E. Moreau, L. Léger, G. Touchard, Effect of a DC surface non-thermal plasma on a flat plate boundary layer for airflow velocity up to 25 m/s, J. Electrostatics 64 (2006) 215–225.
[4] S. Masuda, M. Washizu, Ionic charging of very high resistivity spherical particle, J. Electrostatics 6 (1979) 57–67.
[5] J.R. Roth, D.M. Sherman, Boundary layer flow control with a one atmosphere uniform glow discharge surface plasma, AIAA Paper #98-0328, Reno, Nevada, 1998.
[6] A. Labergue, E. Moreau, N. Zouzou, G. Touchard, Separation control using plasma actuators—application to a free turbulent jet, J. Phys. D 40 (2007) 674–684.
[7] T.C. Corke, C. He, Plasma flaps and slats: an application of weakly-ionized plasma actuators, AIAA Paper #2004-2127, Reno, Nevada, 2004.
[8] T.E. McLaughlin, M.D. Munska, J.P. Vaeth, T.E. Dauwalter, J.R. Goode, S.G. Siegel, Plasma-based actuators for cylinder wake vortex control, AIAA Meeting, Portland, USA, 2004.
[9] M. Forte, J. Jolibois, F. Baudoin, E. Moreau, G. Touchard, M. Cazalens, Optimization of a dielectric barrier discharge actuator and non-stationary measurements of the induced flow velocity—application to airflow control, AIAA Paper #2006-2863, San Francisco, USA, 2006.
[10] C. Louste, G. Artana, E. Moreau, G. Touchard, Sliding discharge in air at atmospheric pressure: electrical behaviour, J. Electrostatics 63 (2005) 615–620.
[11] B. Arad, Y. Gazit, A. Ludmirsky, A sliding discharge device for producing cylindrical shock waves, J. Phys. D 20 (1987) 360–367.
[12] G.N. Tsikrikas, A.A. Serafetinides, The effect of voltage pulse polarity on the performance of a sliding discharge pumped HF laser, J. Phys. D 29 (1996) 2806–2810.